Nitro-Nitrito Photoisomerization of Platinum(II) Complexes with Pt(NO2)42- and (FSO2)2N- Anions: Correlation between Isomerization Ratio and Reaction Cavity

Nakamura, Ibuki

Funasako, Yusuke

Mochida, Tomoyuki

(Citation)
Crystal Growth & Design,20(12):8047-8052

(Issue Date)
2020-12-02

(Resource Type)
journal article

(Version)
Accepted Manuscript

Nitro-Nitrito Photoisomerization of Platinum(II) Complexes with $Pt(NO_2)_4^{2-}$ and $(FSO_2)_2N^-$ Anions: Correlation between Isomerization Ratio and Reaction Cavity

Ibuki Nakamura,[a] Yusuke Funasako,[b] Tomoyuki Mochida*[a,c]

[a]Department of Chemistry, Graduate School of Science, Kobe University, Rokkodai, Nada, Kobe, Hyogo 657-8501, Japan. E-mail: tmochida@platinum.kobe-u.ac.jp

[b]Department of Applied Chemistry Faculty of Engineering, Sanyo-Onoda City University, 1-1-1, Daigakudori, Sanyo-Onoda, Yamaguchi 756-0884, Japan

[c]Center for Membrane Technology, Kobe University Rokkodai, Nada, Kobe, Hyogo 657-8501, Japan

ABSTRACT: Nitro–nitrito linkage isomerization is a well-known photochemical reaction of metal complexes in the solid state. To quantitatively elucidate the influence of the crystal environment on this reaction, we synthesized salts of a cationic platinum(II) nitrito complex with $Pt(NO_2)_4^{2-}$ and $(FSO_2)_2N^-$ anions (**1-Pt(NO$_2$)$_4$** and **1-FSA**, respectively). Their thermal properties and photoreactivities were investigated, and the linkage isomerization of the cations and the $Pt(NO_2)_4$ anion upon ultraviolet photoirradiation at 180 K was observed by X-ray structural analysis. The isomerization levels for the cations in **1-Pt(NO$_2$)$_4$** and **1-FSA** were 49% and 80%, respectively, and that for the $Pt(NO_2)_4$ anion was in the range of 0–65%. The conversion was correlated with the reaction cavity size surrounding the NO_2 ligands.

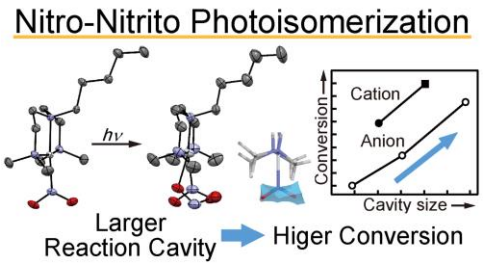

INTRODUCTION

Metal complex photoisomerizations in the solid state have attracted considerable attention over the years.[1,2] To elucidate the isomerization mechanisms, photoexcited metastable states have been structurally analyzed.[3,4,5] A number of metal complexes with a nitrito auxiliary ligand exhibit linkage isomerism, i.e., nitro–nitrito isomerization, in the solid state.[6,7] In these complexes, the thermodynamically stable nitro isomer (nitrito-κ*N*) isomerizes upon ultraviolet (UV) photoirradiation to give the nitrito isomer (nitrito-κ*O*) (Figure 1). This isomerization has also been investigated theoretically.[8] Recently, structural changes occurring in metal complexes upon photoirradiation have been thoroughly examined by Hatcher and Raithby using photocrystallography.[5,9-12] They found that the conversion varies depending on the types of ligands and metals (e.g., M = Ni, Co, Pt, Pd) in the complexes and that some complexes undergo complete photoisomerization. Furthermore, the photoisomerization reaction of some cobalt complexes leads to interesting photomechanical properties as investigated by Boldyreva and Naumov.[13-15] Several studies regarding metal ammine complexes[10,16-19] and organometallic complexes[20] have suggested that the photoreactivity is related to the reaction cavity surrounding the NO_2 ligands. However, factors affecting their photoreactivity have not been fully understood.

In this study, to quantitatively evaluate the effect of the crystalline environment on the photoisomerization of NO_2 complexes, salts containing the cationic Pt^{II} chelate complex $[Pt(L)(NO_2)]^+$ (**1**$^+$; Figure 2a) were synthesized, where the chelating ligand (L) bears a pentyl group. This ligand was selected because of our interest in the thermal properties of ionic liquids containing metal chelate complexes.[21,22] $Pt(NO_2)_4^{2-}$ and $(FSO_2)_2N^-$ (FSA) were used as the counter anions in this study (Figure 2b), and the salts formed using these anions are hereafter designated as **1-Pt(NO$_2$)$_4$** and **1-FSA**, respectively. The FSA anion is often used as the counter anion in ionic liquids.[23] The thermal properties and photoreactivity of the salts were investigated and their isomerization were

monitored by X-ray crystallography. The cation and the $Pt(NO_2)_4^{2-}$ anion exhibited linkage photoisomerization, and their comparison provided insight into the effect of the reaction cavity on the isomerization level. Correlations between the reactivity of complexes and their reaction cavities have been found in various molecular crystals.[24-27]

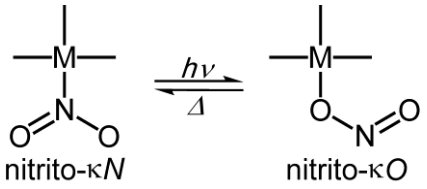

Figure 1. Nitro–nitrito linkage isomerization of metal complexes with a nitrito auxiliary ligand.

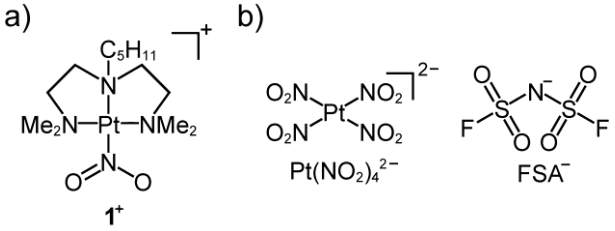

Figure 2. Structures of the (a) cation and (b) anions used in this study.

RESULTS AND DISCUSSION

Thermal Properties. 1-Pt(NO₂)₄ and **1-FSA** were obtained as colorless crystals. Their thermal behaviors were investigated by differential scanning calorimetry (DSC) and thermogravimetry-differential thermal analysis (TG-DTA).

The melting points of **1-Pt(NO₂)₄** and **1-FSA** were 459.5 K and 392.6 K, respectively (Table 1). It is reasonable that the divalent salt has a higher melting point, due to its stronger electrostatic interactions. The DSC traces are shown in Figure S1 (Supporting Information). Upon cooling from the melt, **1-Pt(NO₂)₄** exhibited a glass transition at 333 K, whereas **1-FSA** exhibited partial crystallization, and the remaining liquid exhibited a glass transition at 280 K. The ratios of the glass transition temperature to the melting point (T_g/T_m) for these salts were 0.72 and 0.71, respectively,

which are comparable to the typical values for molecular liquids (T_g/T_m = 2/3).[28] No solid phase transitions were observed down to 123 K in both salts.

The TG traces of the salts are shown in Figure 3. The decomposition temperatures (the 3 wt% weight loss temperatures) of **1-Pt(NO$_2$)$_4$** and **1-FSA** were 496 and 523 K, respectively (Table 1). In the DTA trace of each salt, a large exothermic peak was observed at their respective decomposition temperatures. **1-Pt(NO$_2$)$_4$** exhibited a steep weight loss of ~30 wt%, and its lower decomposition temperature may be ascribed to its nitro groups in the anion. **1-FSA** exhibited a higher decomposition temperature and a two-step weight loss. The first step (~10 wt%, 510–530 K) corresponded to the loss of the NO_2 ligand (calculated value 7%) and the second step likely included the loss of the chelating ligand (~40 wt%, calculated value 35 wt%).

Table 1. Melting points (T_m), melting enthalpies (ΔH_m), glass transition temperatures (T_g), and decomposition temperatures (T_{dec}) of the salts synthesized in this study

Salt	T_m (K)	ΔH_m(kJ mol^{-1})	T_g (K)	T_g/T_m	T_{dec}[a] (K)
1-Pt(NO$_2$)$_4$	459.5	68.1	333	0.72	496
1-FSA	392.6	29.6	280	0.71	523

[a]Determined by thermogravimetric (TG) analysis (3 wt% weight loss temperature, measured at 3 K min^{-1} under a nitrogen atmosphere).

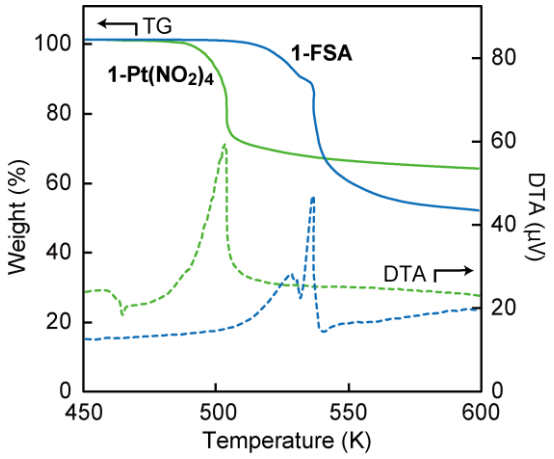

Figure 3. Thermogravimetry-differential thermal analysis (TG–DTA) traces of **1-Pt(NO$_2$)$_4$** (green line) and **1-FSA** (blue line) measured under a nitrogen atmosphere at 3 K min^{-1}. The TG and DTA curves are represented by solid and dashed lines, respectively.

Spectral Investigation of Photoisomerization. Investigation by IR spectroscopy revealed photoisomerization in both salts at 180 K. The IR spectra of the polycrystalline samples before and after UV photoirradiation (365 nm, LED) at 180 K are shown in Figure S2 (Supporting information). Upon photoirradiation of **1-FSA**, strong and weak peaks for nitrito–κ*O* stretching vibrations appeared at 1080 and 1425 cm^{-1}, respectively, and the intensity of the nitrito–κ*N* stretching vibration peak at 1320 cm^{-1} decreased. These spectral changes indicate the occurrence of linkage isomerization.[29] **1-Pt(NO$_2$)$_4$** also exhibited the appearance of peaks at 1080 and 1430 cm^{-1}, whereas no clear changes were observed around 1320 cm^{-1} due to overlap of the peaks. In both cases, the original spectrum was recovered when the sample was warmed to 300 K, indicating efficient thermal relaxation. Photoirradiation at 300 K caused no spectral changes.

Additionally, the UV-vis spectra of these salts were measured in solution (Figure S3, supporting information). **1-Pt(NO$_2$)$_4$** exhibited a shoulder at 315 nm (ε = 917 M^{-1}cm^{-1}) in acetonitrile, whereas **1-FSA** exhibited a peak at 301 nm (ε = 293 M^{-1}cm^{-1}) in dichloromethane. Their absorption coefficients at 365 nm were 177 and 37 M^{-1}cm^{-1}, respectively. These small values indicate that the effect of surface absorption is not significant in the case of crystal photoirradiation at 365 nm.

Crystal Structures before Photoirradiation. The crystal structures of **1-Pt(NO$_2$)$_4$** and **1-FSA** were determined at 180 K before photoirradiation. These salts crystallized in the *C*2/*c* and *P*2$_1$/*n* space groups, respectively (*Z* = 4), and their packing diagrams are shown in Figure 4. The anion in **1-FSA** is located near the coordination plane of the cation. The structures were also determined at

100 K, but no significant structural changes were observed.

The molecular structures of each of the cations in these salts (Figure 5) had a planar, four-coordinate structure with a nitrito–κ*N* coordination. The cations have almost identical geometries, exhibiting a Pt–N_{NO2} bond length of 2.005(2) Å and a dihedral angle between the coordination plane and the NO_2 ligand of approximately 80° (Table S1, Supporting Information). The pentyl substituent in each cation adopted the all-*trans* conformation without disorder.

The anion in **1-Pt(NO₂)₄** was located on a crystallographic 2-fold axis (Figure 6a, left) and had a planar structure with a nitrito–κ*N* coordination. The Pt–N_{NO2} bond lengths were 2.012(3), 2.014(3), and 2.032(5) Å, which are significantly longer than those in the cations. Furthermore, the dihedral angles between the coordination plane and the NO_2 ligands varied: 26° (N5 and N5), 67° (N6), and 71° (N7). The geometry of the cation is similar to that of other reported salts, although only a few crystal structures containing $[Pt(NO_2)_4]^{2-}$ are known.[30]

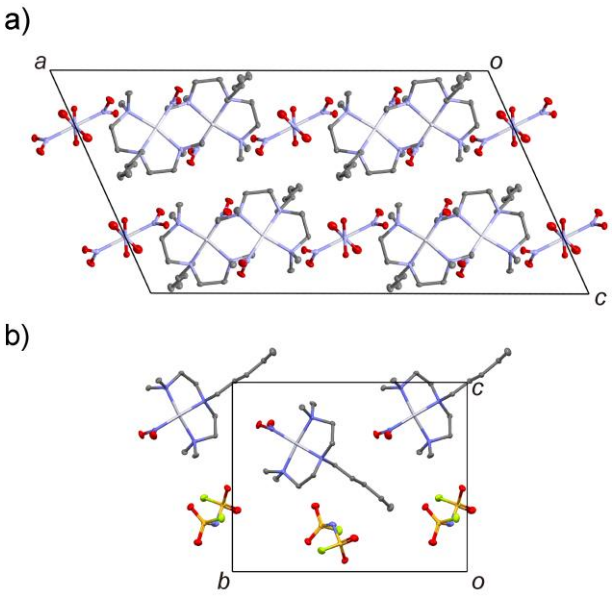

Figure 4. Packing diagrams of (a) **1-Pt(NO₂)₄** and (b) **1-FSA** at 100 K. The hydrogen atoms have been omitted for clarity.

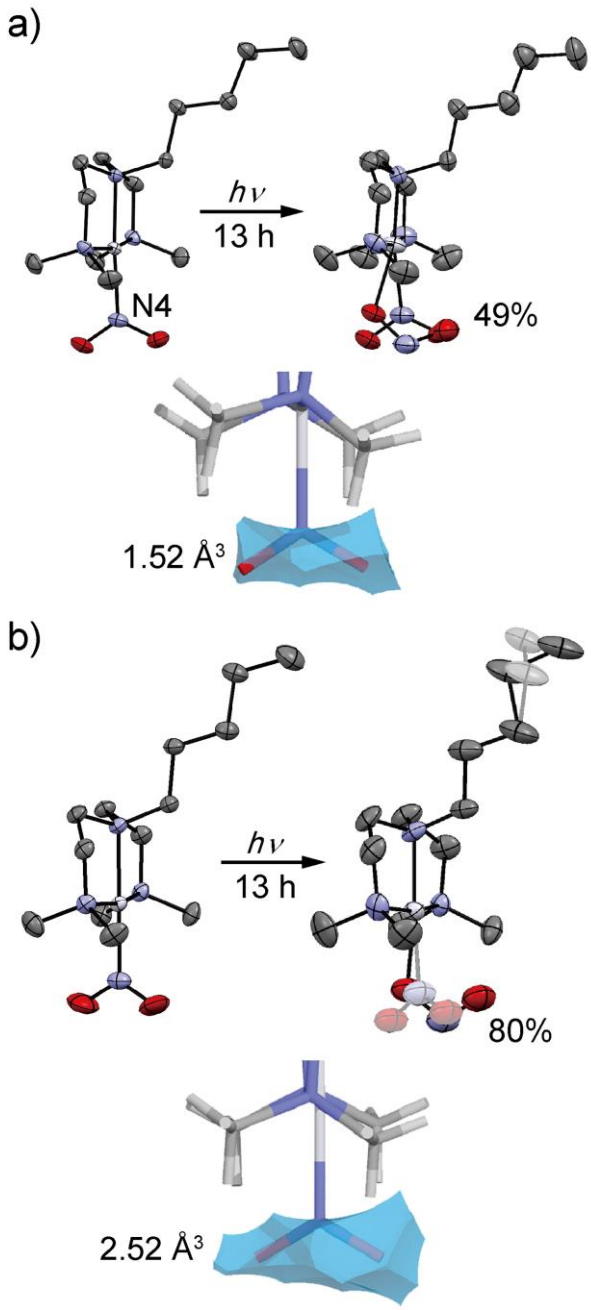

Figure 5. Molecular structures of the cations in (a) **1-Pt(NO$_2$)$_4$** and (b) **1-FSA** at 180 K before and after photoirradiation for 13 h. The hydrogen atoms have been omitted for clarity, and the disordered parts are shown in gray. The populations of the nitrito-κ*O* isomers (%) are shown in each figure. The reaction cavity surrounding the NO_2 ligand and its volume are also shown below each figure.

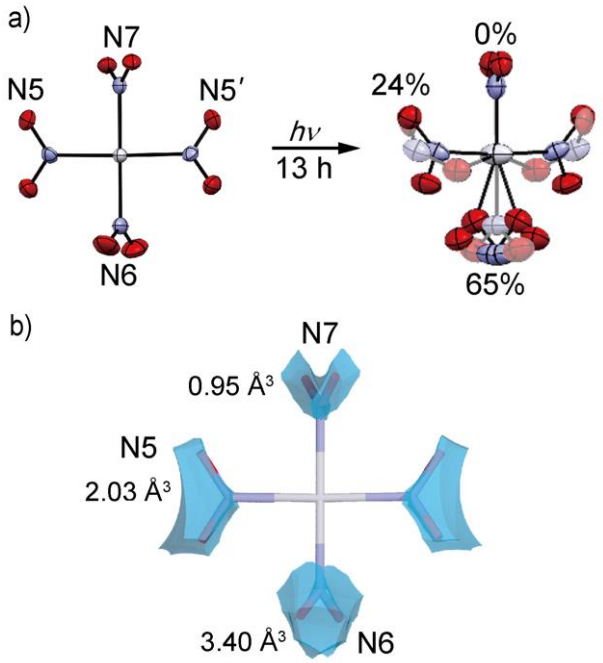

Figure 6. (a) Molecular structures of the anion in **1-Pt(NO₂)₄** at 180 K before and after photoirradiation for 13 h. The lower occupancy moieties in the disordered parts are shown in gray. The populations of the nitrito-κ*O* isomers (%) are shown. (b) Reaction cavities surrounding the NO_2 ligands and their volumes.

Crystal Structures after Photoirradiation. The structures of the salts were determined at 180 K after photoirradiation for 1, 4, and 13 h. Isomerization of the cation in each salt and the anion in **1-Pt(NO₂)₄** was observed.

The molecular structures of the cations after photoirradiation for 13 h were also evaluated (Figure 5). Upon photoirradiation, the nitrito ligands exhibited disorder and the population of the *endo*-nitrito-κ*O* isomer increased. The conversions for **1-Pt(NO₂)₄** and **1-FSA** were 49% and 80%, respectively. In addition, photoirradiation of **1-FSA** caused a two-fold disorder of the pentyl group of the cation (0.35:0.67 occupancy) with the population of the new conformer predominating.

The anion in **1-Pt(NO₂)₄** also exhibited photoisomerization (Figure 6a), where the conversions

of the crystallographically independent NO_2 ligands were different: 65% (N7), 24% (N5 and N5), and 0% (N6). There was no correlation between the dihedral angle and observed conversion. The sum of the conversion in the anion was 113%, which roughly corresponds to the isomerization of a nitro ligand into a nitrito linkage in the anion. Solid-state photoisomerization of complexes with more than three nitrito ligands has not been reported to date, although the photoisomerization of several complexes containing two nitrito ligands has been described.[9,10]

The populations of the nitrito-κ*O* isomer at each site in the cations and the $Pt(NO_2)_4$ anion were plotted as a function of irradiation time (Figure 7). The conversion for the cations became almost constant after 4 h. The differences in the quantum yields of isomerization between the cation and anion may kinetically affect the initial isomerization rate, but this does not affect the final conversion. To investigate whether thermal relaxation occurred, the samples were left in the dark for another 4 h at 180 K after the 13 h data were collected and the structures were determined again. The analysis showed an unchanged population of the isomer (< 1.2% change), indicating negligible thermal relaxation.

A slight expansion of the unit cell volume was observed in each salt upon photoisomerization, similar to other salts with nitrito ligands owing to the larger size of the nitrito-*κO* isomer.[9,11] The unit cell volumes of **1-Pt(NO$_2$)$_4$** and **1-FSA** at 180 K increased by 1.1% and 1.8%, respectively, after 13 h of photoirradiation. The smaller cell expansion of **1-Pt(NO$_2$)$_4$** compared to **1-FSA** may be ascribed to the stronger Coulombic interactions in the divalent salt.

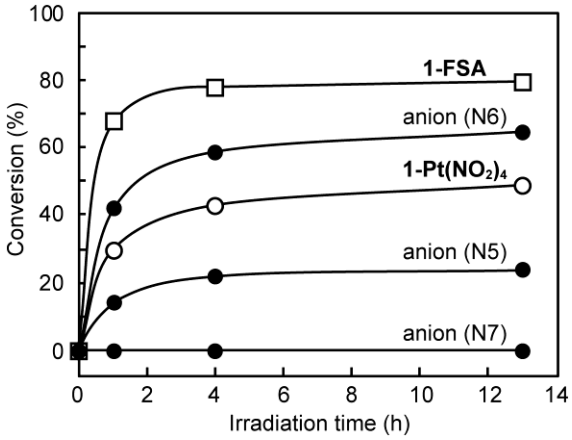

Figure 7. (a) Plot of conversion versus photoirradiation time at 180 K for the NO_2 ligands in **1-Pt(NO$_2$)$_4$** (○, cation; ●, anion) and **1-FSA** (□).

Correlation between Photoreactivity and Reaction Cavities. To understand the effect of the crystal environment on linkage isomerization, the reaction cavities surrounding the nitrito ligands were calculated and the cavity volume was found to affect the conversion.

The calculated reaction cavities and their volumes in the salts at 180 K are shown in Figures 5 and 6, and are also given in Table S2 (Supporting Information). The reaction cavity, calculated for the structure before photoirradiation, is defined as the space surrounded by the spheres of atoms surrounding the ligand, the radus of the sphere being greater by 1.2 Å than the van der Waals radus of the corresponding atom.[25] The conversions after 13 h of photoirradiation at 180 K were plotted versus the reaction cavity volume (Figure 8). The conversions for both the cation and anions were seen to increase with increasing reaction cavity volume, indicating a correlation between the two parameters. Furthermore, the anion exhibited a conversion lower than that of the cation for the same reaction cavity volume. This suggests that anion isomerization requires a reaction cavity larger than that required by cation isomerization, which is supported by DFT calculations. The calculated Pt–$X_{nitrito}$ distances (X = N, O) in the nitrito-κ*N* and -κ*O* isomers of the cation were 2.022 and 2.045 Å,

respectively, whereas those in the $Pt(NO_2)_4^{2-}$ anion were 2.056 and 2.106 Å, respectively (Figure S4, Supporting Information). The significantly longer bond lengths in the anion, especially those of the -κ*O* isomer, confirm that the anion requires a reaction volume larger than that of the cation.

The trend of conversion in each site is therefore consistent with the reaction cavity volume. This suggests that the conversion is thermodynamically limited by the reaction cavity volume, because the ligand volume expands upon isomerization, though not only the size but also the shape of the cavity may affect the conversion. The isomerization of each ligand should occur independently, because each NO_2 ligand in both salts has no contacts with other NO_2 ligands in the crystal. The effect of the multiple NO_2 ligands in the anion, whose isomerizations might interfere with each other, may be a subject of further study.

Additionally, the reaction cavity around the pentyl substituent of the cations at 180 K was examined. The substituent in **1-FSA** was disordered upon photoirradiation (Figure 5b, middle). The reaction cavity volumes surrounding the $-CH_2CH_3$ moiety in **1-Pt(NO₂)₄** and **1-FSA** were 3.5 and 8.7 $Å^3$, respectively, and the large space in **1-FSA** may be related to its disorder. The pentyl substituent in **1-FSA** has no contact with the NO_2 ligand, hence the disorder is not a direct consequence of the photoisomerization.

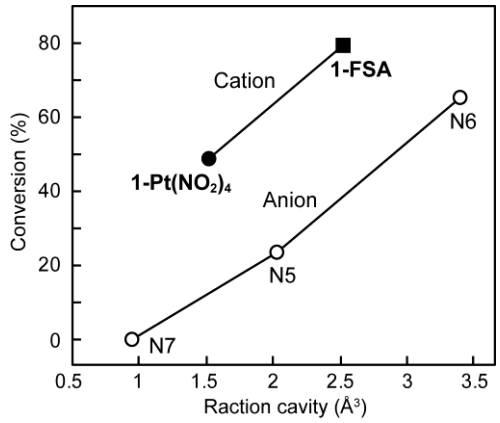

Figure 8. Correlation between the reaction cavity volume and conversion (180 K, after 13 h

photoirradiation).

CONCLUSION

We synthesized salts of cationic platinum chelate complexes bearing an NO_2 auxiliary ligand and elucidated their nitro–nitrito photoisomerization behavior by X-ray crystallography. In addition to the cation, the $Pt(NO_2)_4^{2-}$ anion also exhibited photoisomerization, which is the first example of the photoisomerization of a complex having more than three NO_2 ligands. Comparing the salts enabled the correlation between their conversion levels and reaction cavity volumes to be quantitatively examined. The conversion increased with an increase in the reaction cavity volume, whereas the isomerization levels for the cation and anions differed due to their different reaction volumes. In a subsequent paper, we further discuss the effect of packing efficiency on the photoisomerization reaction.

EXPERIMENTAL SECTION

General Considerations. 3-Pentyl-1,5-diphthalimido-3-azapentane was prepared according to the literature.[31] ^1H NMR spectra were recorded using a Bruker Avance 400 instrument. Room temperature FT-IR spectra were measured using a Thermo Scientific Nicolet iS5 FT-IR spectrometer attached to an ATR unit (diamond). Variable temperature IR spectra were recorded for samples sandwiched between CaF_2 plates using a JASCO FT/IR-4700 spectrometer. Temperature control was performed using the UNISOKU CoolSpeK UV USP-203-A cryostat. DSC measurements were performed using a TA Q100 differential scanning calorimeter at a scan rate of 10 K min^{-1}. TG-DSC measurements were performed using a Rigaku TG8120 thermal analyzer at a scan rate of 3 K min^{-1} under a nitrogen atmosphere. ESI-MS spectra were recorded using a Thermo Fisher Scientific LTQ-

Orbitrap Discovery spectrometer. UV photoirradiation was carried out using a Hamamatsu LC-L1 V3 lightning cure UV-LED (365 nm). The packing indices were calculated using Platon.[32] The reaction cavities were calculated using the Cavity v5.0 program.[25] DFT calculations were performed with Spartan '18 (Wave function Inc.) at the ωB97-D/LanL2DZ level.

Synthesis of 1,1,7,7-Tetramethyl-4-pentyldiethylenetriamine (L). Under a nitrogen atmosphere, 3-pentyl-1,5-diphthalimido-3-azapentane (3.03 g, 7.00 mmol) and hydrazine monohydrate (7.11 g, 142 mmol) were dissolved in ethanol (30 mL) and refluxed for 1 day. The solution was filtered, and the filtrate was evaporated under reduced pressure. The residue was dissolved in chloroform and the solution stirred at room temperature for 19 h. The solution was filtered, and the filtrate was evaporated to give 4-pentyldiethylenetriamine as a yellow liquid (yield 1.12 g, 93%). ^{1}H NMR (400 MHz, $CDCl_3$): δ = 2.74 (t, J = 6.0 Hz, 4H, $H_{1,5}$), 2.49 (t, J = 6.0 Hz, 4H, $H_{2,4}$), 2.42 (t, J = 7.4 Hz, 2H, $H_{1'}$), 1.48–1.21 (m, 6H, $H_{2',3',4'}$), 0.89 (t, J = 7.1 Hz, 3H, $H_{5'}$). Under a nitrogen atmosphere, formic acid (4.4 mL, 117 mmol) was added dropwise to a mixture of 4-pentyldiethylenetriamine (1.12 g, 6.48 mmol) and formaldehyde (35% aqueous solution, 9 mL, 120 mmol) in an ice bath, and the resulting solution was refluxed for 40 h. The solution was made basic (pH 10) at room temperature using 2 M aqueous NaOH and extracted with diethyl ether (25 mL × 4). The organic layer was dried over $MgSO_4$ and filtered, and the filtrate was evaporated to give a yellow liquid. Chloroform and activated carbon were added to the liquid, and the mixture was boiled for 3 min and filtered. The filtrate was evaporated to give 1,1,7,7-tetramethyl-4-pentyldiethylenetriamine as a yellow liquid (yield 1.08 g, 73%). ^{1}H NMR (400 MHz, $CDCl_3$): δ = 2.58 (t, J = 7.3 Hz, 4H, $H_{2,6}$), 2.45 (t, J = 7.7 Hz, 2H, $H_{1'}$), 2.38 (t, J = 7.4 Hz, 4H, $H_{3,5}$), 2.23 (s, 12H, $H_{1,7}$), 1.45 (quin, J = 7.6 Hz, 2H, $H_{2'}$), 1.31 (quin, J = 7.1 Hz, 2H, $H_{3'}$), 1.25 (sext, J = 7.1 Hz, 2H, $H_{4'}$), 0.89 (t, J = 3.7 Hz, 3H, $H_{5'}$).

Synthesis of $[Pt(L)(NO_2)]_2[Pt(NO_2)_4]$ (1-$Pt(NO_2)_4$). An aqueous solution (1.5 mL) of

$K_2[Pt(NO_2)_4]$ (89 mg, 0.20 mmol) was added to an acetone solution (0.3 mL) of **L** (22.4 mg, 0.098 mmol) and stirred at 70 °C for 22 h. After evaporation of acetone, the solution was extracted with dichloromethane (5 mL × 4). The organic layer was dried over $MgSO_4$ before being evaporated. The orange residue was dissolved in a small amount of acetonitrile in a test tube, and diethyl ether was then slowly layered onto the solution. Pale yellow block crystals were obtained by storing the solution at –4 °C for 3 days (yield 27 mg, 21%). ^{1}H NMR (400 MHz, CD_3CN): δ = 2.58 (t, J = 7.3 Hz, 4H, $H_{2,6}$), 2.45 (t, J = 7.7 Hz, 2H, $H_{1'}$), 2.38 (t, J = 7.4 Hz, 4H, $H_{3,5}$), 2.23 (s, 12H, $H_{1,7}$), 1.45 (quin, J = 7.6 Hz, 2H, $H_{2'}$), 1.31 (quin, J = 7.1 Hz, 2H, $H_{3'}$), 1.25 (sext, J = 7.1 Hz, 2H, $H_{4'}$), 0.89 (t, J = 3.7 Hz, 3H, $H_{5'}$). FT-IR (ATR, cm^{-1}): 2930, 2870 (C-H), 1375, 1338 (NO_2). Anal. Calcd. for $C_{26}H_{62}N_{12}O_{12}Pt_3$: C, 23.66; H, 4.73; N, 12.73. Found: C, 23.80; H, 4.11; N, 12.80.

Synthesis of [Pt(L)(NO_2)][FSA] (1-FSA). An aqueous solution (0.3 mL) of K[FSA] (31.6 mg, 0.14 mmol) was added to an acetone solution (0.6 mL) of [Pt(L)(NO_2)][PF_6] (40 mg, 0.065 mmol), which had been prepared from **1-Pt(NO_2)$_4$** by the addition of KPF_6. The solution was stirred at room temperature for 2 h. After evaporation of acetone, the solution was extracted with dichloromethane (5 mL × 6). The organic layer was washed with water (10 mL × 2) and evaporated. The anion exchange procedure was repeated again, at which point the complete disappearance of PF_6^- was confirmed by ^{19}F NMR spectra (CD_3CN). The resulting colorless oil was dissolved in a small amount of methanol in a test tube, and diethyl ether was then slowly layered onto the solution. Colorless needle crystals were obtained by storing the solution at –4 °C for 3 days (yield 23 mg, 58%). ^{1}H NMR (400 MHz, CD_3CN): δ = 3.44–3.25 (m, 4H, $H_{2,6,1'}$), 3.05–2.95 (m, 10H, $H_{3,5,7}$), 2.81–2.72 (m, 6H, H_1), 1.55–1.47 (m, 2H, $H_{2'}$), 1.42–1.31 (m, 2H, $H_{3',4'}$), 0.95 (t, J = 0.71 Hz, 3H, $H_{5'}$). FT-IR (ATR, cm^{-1}): 2949, 2868 (C-H), 1375, 1336 (NO_2). Anal. Calcd. for $C_{13}H_{31}F_2N_5O_6PtS_2$: C, 24.00; H, 4.80; N, 10.76. Found: C, 24.00; H, 4.72; N, 10.77.

X-ray Crystallography. Data were collected using a Bruker APEX II Ultra with MoKα

radiation at 100 and 180 K. The structural changes after photoirradiation (365 nm, 45 mW/cm^2) were investigated at 180 K. The measurements were performed on the same crystal for each salt. The crystals were rotated intermittently during photoirradiation, and diffraction data were collected in the dark within 2 h. The structures were solved by the direct method using SHELXL.[33] The crystallographic parameters are provided in Tables S3 and S4.

ASSOCIATED CONTENT

Supporting Information

DSC traces (Figure S1), IR spectra before and after photoirradiation (Figure S2), UV spectra in solution (Figure S3), DFT calculations (Figure S4), bond lengths and dihedral angles (Table S1), reaction cavity volumes (Tables S2), and crystallographic tables (Tables S3 and S4). This information is available free of charge via the internet at http://pubs.acs.org/.

Accession Codes

CCDC- 2032450 (**1-Pt(NO$_2$)$_4$**, 100 K), 2032451 (**1-Pt(NO$_2$)$_4$**, 180 K), 2032452 (**1-Pt(NO$_2$)$_4$**, 180 K, after 13 h photoirradiation), 2032453 (**1-FSA**, 100 K), 2032454 (**1-FSA**, 180 K), and 2032455 (**1-FSA**, 180 K, after 13 h photoirradiation) contain the supplementary crystallographic data for this paper. These data can be obtained free of charge from The Cambridge Crystallographic Data Centre via www.ccdc.cam.ac.uk/data_request/cif.

AUTHOR INFORMATION

Corresponding Author

*E-mail: tmochida@platinum.kobe-u.ac.jp. Tel/Fax: +81-78-803-5679.

ORCID

Tomoyuki Mochida: 0000-0002-3446-2145

Yusuke Funasako: 0000-0002-1523-9730

Notes

The authors declare no competing financial interest.

ACKNOWLEDGMENTS

We thank Mr. Ryo Sumitani (Kobe University) for his help with the crystallographic analysis. This work was financially supported by KAKENHI (grant number 20H02756) from the Japan Society for the Promotion of Science (JSPS).

REFERENCES

(1) Vittal, J.J.; Quah, H. S. Photochemical reactions of metal complexes in the solid state. *Dalton Trans*. **2017**, *46*, 7120–7140.

(2) Simmons, E.L.; Wendlandt, W.W. Solid-state photochemical reactions of transition-metal coordination compounds. *Coord. Chem. Rev*. **1971**, *7*, 11–27.

(3) Coppens, P.; Novozhilova, I.; Kovalevsky, A. Photoinduced Linkage Isomers of Transition-Metal Nitrosyl Compounds and Related Complexes. *Chem. Rev*. **2002**, *102*, 861–884.

(4) Coppens, P.; Vorontsov, I. I.; Graber, T.; Gembickya, M.; Kovalevskya, A. Yu. The structure of short-lived excited states of molecular complexes by time-resolved X-ray diffraction. *Acta Crystallogr. Sect. A* **2005**, *61*, 162–172.

(5) Hatcher, L. E.; Skelton, J. M.; Warren, M. R.; Raithby, P. R. Photocrystallographic Studies on Transition Metal Nitrito Metastable Linkage Isomers: Manipulating the Metastable State. *Acc.*

Chem. Res. **2019***, 52*, 1079–1088.

(6) Grenthe, I.; Nordin, E. Nitrito-nitro linkage isomerization in the solid state. 2. A comparative study of the structures of nitrito- and nitropentaaminecobalt(III) dichloride. *Inorg. Chem*. **1979**, *18*, 1869–1874.

(7) Awasabisah, D.; Richter-Addo, G.B. NO_x Linkage Isomerization in Metal Complexes, *Adv. Inorg. Chem.* **2015**, *67*, 1–78.

(8) Muya, J. T.; Chung, H.; Lee, S. U. Theoretical investigation on the ground state properties of the hexaamminecobalt(III) and nitro–nitrito linkage isomerism in pentaamminecobalt(III) in vacuo. *RSC adv.* **2018**, *8*, 3328–3342.

(9) Warren, M. R.; Brayshaw, S. K.; Hatcher, L. E.; Johnson, A. L.; Schiffers, S.; Warren, A. J.; Teat, S. J.; Warren, J. E.; Woodall, C. H.; Raithby, P. R. Photoactivated linkage isomerism in single crystals of nickel, palladium and platinum di-nitro complexes – a photocrystallographic investigation. *Dalton Trans*. **2012**, *41*, 13173–13179.

(10) Hatcher, L. E. Raising the (metastable) bar: 100% photo-switching in $[Pd(Bu_4dien)(\eta^1\text{-}\underline{N}O_2)]^+$ approaches ambient temperature. *CrystEngComm* **2016**, *18*, 4180–4187.

(11) Hatcher, L. E.; Raithby, P. R. The impact of hydrogen bonding on 100% photo-switching in solid-state nitro–nitrito linkage isomers. *CrystEngComm* **2017**, *19*, 6297–6304.

(12) Hatcher, L. E.; Skelton, J. M.; Warren, M. R.; Stubbs, C.; Lora da Silva, E.; Raithby, P. R. Monitoring photo-induced population dynamics in metastable linkage isomer crystals: a crystallographic kinetic study of $[Pd(Bu_4dien)NO_2]BPh_4$. *Phys. Chem. Chem. Phys*. **2018**, *20*, 5874–5886.

(13) Naumov, P. N; Chizhik, S.; Panda, M. K.; Nath, N. K.; Boldyreva, E., Mechanically Responsive Molecular Crystals. *Chem. Rev*. **2015**, *115*, 12440–12490.

(14) Chizhik, S.; Sidelnikov, A.; Zakharov, B.; Naumov, P.; Boldyreva, E. Quantification of

photoinduced bending of dynamic molecular crystals: from macroscopic strain to kinetic constants and activation energies. *Chem. Sci*. **2018**, *9*, 2319–2335.

(15) Naumov, P.; Sahoo, S. C.; Zakharov, B. A.; Boldyreva, E. V. Dynamic Single Crystals: Kinematic Analysis of Photoinduced Crystal Jumping (The Photosalient Effect). *Angew. Chem., Int. Ed*. **2013**, *52*, 9990−9995.

(16) Sidelnikov, A. A.; Chizhik, S. A.; Zakharov, B. A.; Chupakhin, A. P.; Boldyreva, E. V. The effect of thermal expansion on photoisomerisation in the crystals of $[Co(NH_3)_5NO_2]Cl(NO_3)$: different strain origins – different outcomes. *CrystEngComm* **2016**, *18*, 7276–7283.

(17) Boldyreva, E.V. Crystal-Structure Aspects of Solid-State Inner-Sphere Isomerization in Nitro(nitrito)pentaamminecobalt(III) Complexes. *Russ. J. Coord. Chem.* **2001**, *27*, 297–323.

(18) Ohba, S.; Tsuchimoto, M.; Kurachi, S. Investigation of solid-state photochemical nitro–nitrito linkage isomerization: crystal structures of trans-bis-(ethyl-enedi-amine)(iso-thio-cyanato)-nitritocobalt(III) salts: thio-cyanate, chloride monohydrate, and perchlorate–thio-cyanate-(0.75/0.25). *Acta Crystallogr., Sect. E*, **2018**, *74*, 1526–1531.

(19) Kubota, M.; Ohba, S. Nitro-nitrito linkage photoisomerization in crystals of pentaamminenitrocobalt(III) dichloride. *Acta Crystallogr. Sect. B*. **1992**, *48*, 627–632.

(20) Kutniewska, S. E.; Kamiński, R.; Buchowicz, W.; Jarzembska, K. N. Photo- and Thermoswitchable Half-Sandwich Nickel(II) Complex: $[Ni(\eta^5\text{-}C_5H_5)(IMes)(\eta^1\text{-}NO_2)]$. *Inorg. Chem*. **2019**, *58*, 16712–16721.

(21) Cho, S.; Mochida, T. Thermal properties and crystal structures of rhenium(I) carbonyl complexes with tridentate ligands: Preparation of rhenium-containing ionic liquids. *Inorg. Chem*. **2020**, *59*, 847–853.

(22) Funasako, Y.; Mochida, T.; Takahashi, K.; Sakurai, T.; Ohta, H. Vapochromic Ionic Liquids

from Metal-Chelate Complexes Exhibiting Reversible Changes in Color, Thermal and Magnetic Properties. *Chem. Eur. J*. **2012**, *18*, 11929–11936.

(23) Kar, M.; Matuszek, K.; MacFarlane, D.R. Ionic liquids. *Kirk-Othmer Encyclopedia of Chemical Technology*, John Wiley & Sons, Inc., Hoboken, **2019**.

(24) Ohashi, Y. Crystalline State Photoreactions: Direct Observation of Reaction Processes and Metastable Intermediates; Springer: Tokyo, Japan, **2014**.

(25) Ohashi, Y.; Yanagi, K.; Kurihara, T.; Sasada, Y.; Ohgo, Y. Crystalline state reaction of cobaloxime complexes by X-ray exposure. 1. A direct observation of Co−C bond cleavage in [(R)-1-cyanoethyl][(*S*)-(−)-α-methylbenzylamine]bis-(dimethylglyoximato)cobalt(III). *J. Am. Chem. Soc*. **1981**, *103*, 5805−5812.

(26) Yamazaki, Y.; Sekine, A.; Uekusa, H. In Situ Control of Photochromic Behavior through Dual Photo-Isomerization Using Cobaloxime Complexes with Salicylidene-3-aminopyridine and 3-Cyanopropyl Ligands. *Cryst. Growth Des*. **2017**, *17*, 19−27.

(27) Funasako, Y.; Ason, M.; Takebayashi, J.-i.; Inokuchi, M. Solid-State Photochromism of Salts of Cationic Spiropyran with Various Anions: A Correlation between Reaction Cavity Volumes and Reactivity. *Cryst. Growth Des*. **2019**, *19*, 7308–7314.

(28) Turnbull, D.; Cohen, M. H. *Crystallization Kinetics and Glass Formation* in *Modern Aspect of the Vitreous State*, ed. J. D. MacKenzie, Butterworth & Co. Publishers Ltd., London, vol. 1, **1960**.

(29) Penland, R. B.; Lane, T. J.; Quagliano, J. V. *J. Am. Chem. Soc.* **1956**, *78*, 887–889.

(30) Khranenko, S. P.; Kuratieva, N. V.; Gromilov, S. A. Crystal structures of [*M*En$_2$][Pt(NO$_2$)$_4$] (*M* = Cu, Pd). *J. Struct. Chem.* **2014**, *55*, 306–310.

(31) Miranda, C., Escartí, F., Lamarque, L., Yunta, M. J. R., Navarro, P., García-España, E., Jimeno, M. L. New ^{1}H-pyrazole-containing polyamine receptors able to complex L-glutamate in water at physiological pH values. *J. Am. Chem. Soc*. **2004**, *126*, 823–833.

(32) Spek, A. L. Structure validation in chemical crystallography. *Acta Crystallogr., Sect. D: Biol. Crystallogr*. **2009**, *65*, 148–155.

(33) Sheldrick, G. M. A short history of *SHELX*. *Acta Crystallogr., Sect. A: Found. Crystallogr*. **2008**, *64*, 112−122.

Supporting Information

Nitro-Nitrito Photoisomerization of Platinum(II) Complexes with $Pt(NO_2)_4^{2-}$ and $(SO_2F)_2N^-$ anions: Correlation between Isomerization Ratio and Reaction Cavity

Ibuki Nakamura,[a] Yusuke Funasako,[b] Tomoyuki Mochida*[a,c]

[a]*Department of Chemistry, Graduate School of Science, Kobe University, Rokkodai, Nada, Kobe, Hyogo 657-8501, Japan. E-mail: tmochida@platinum.kobe-u.ac.jp*

[b]*Department of Applied Chemistry Faculty of Engineering, Sanyo-Onoda City University, 1-1-1, Daigakudori, Sanyo-Onoda, Yamaguchi 756-0884, Japan*

[c]*Center for Membrane Technology, Kobe University, Rokkodai, Nada, Kobe, Hyogo 657-8501, Japan*

Contents

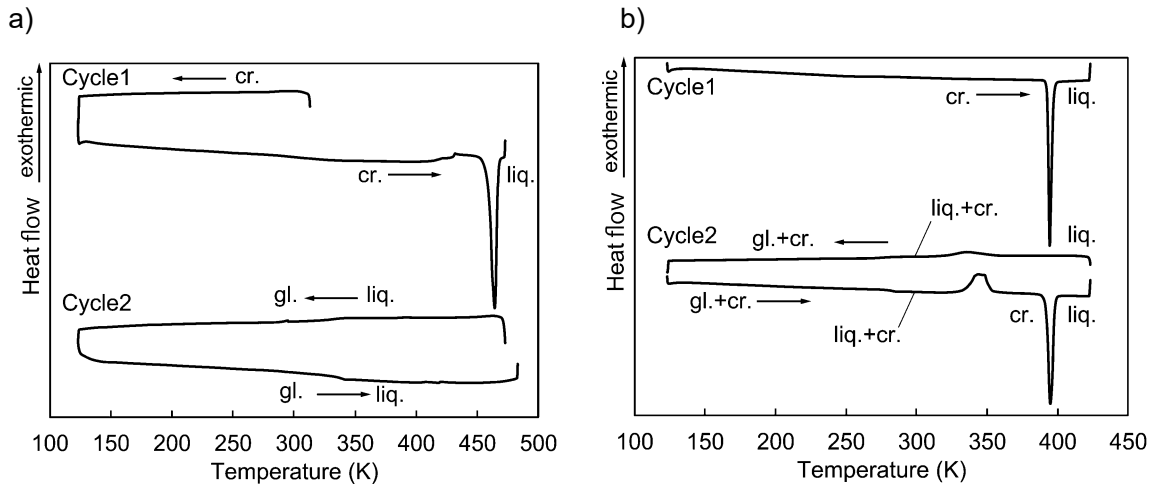

Figure S1. DSC traces of (a) **1-Pt(NO$_2$)$_4$** and (b) **1-FSA** measured at 10 K min^{-1}, where cr., liq., and gl. stand for the crystal state, liquid state, and glassy state, respectively.

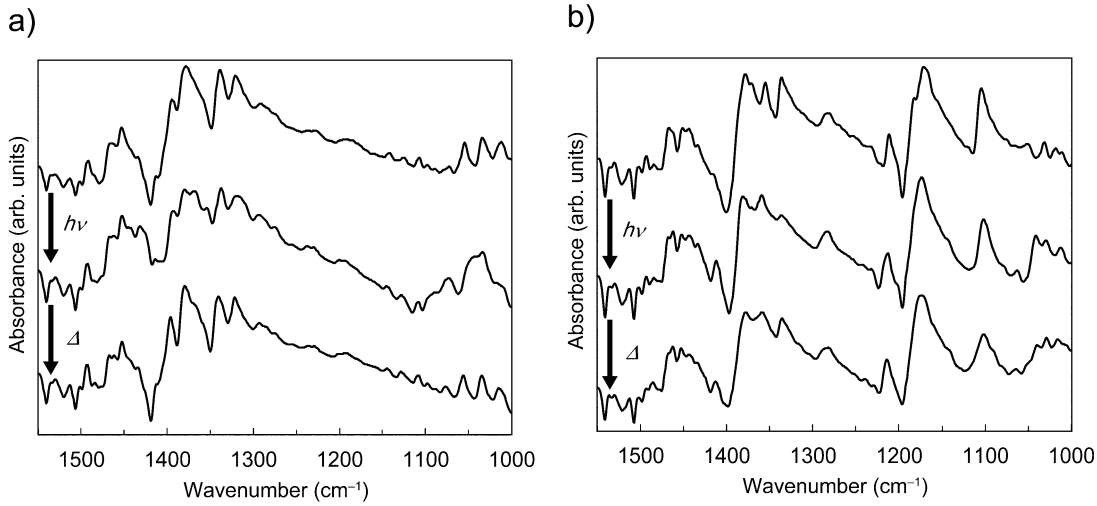

Figure S2. FT-IR spectra of (a) **1-Pt(NO$_2$)$_4$** and (b) **1-FSA**. Before photoirradiation (180 K, top), after photoirradiation for 1 h (180 K, middle), and after returning to 300 K (bottom).

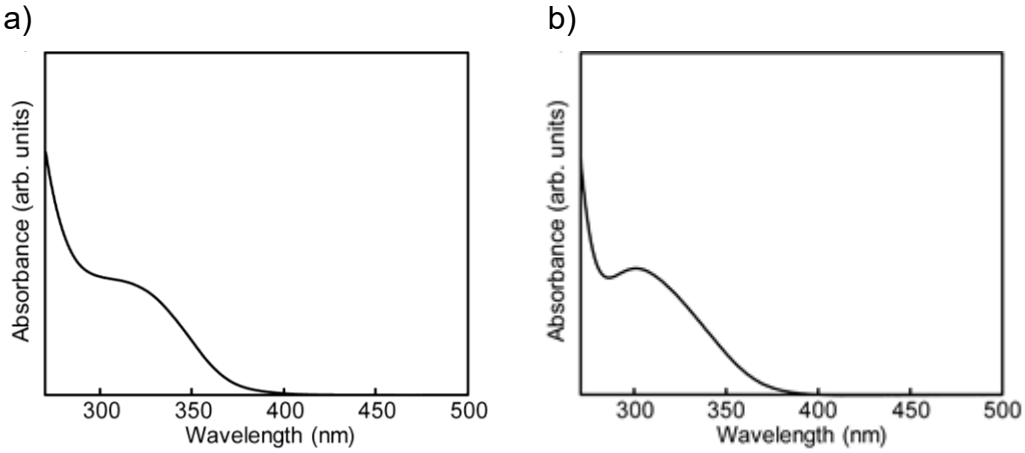

Figure S3. UV-Vis spectra of (a) **1-Pt(NO$_2$)$_4$** (acetonitrile) and (b) **1-FSA** (dichloromethane).

a) $[PtL(NO_2)]^+$ b) $[Pt(NO_2)_4]^{2-}$

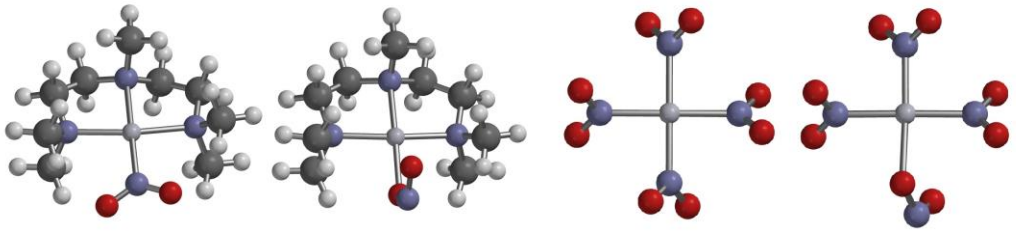

	nitrito-κ*N*	nitrito-κ*O*	nitrito-κ*N*	nitrito-κ*O*
E /au	−844.9663	−844.9607	−939.4513	−939.4446
G^0 /au	−844.6824	−844.6793	−939.4550	−939.4495

Figure S2. DFT calculations (ωB97-D/LanL2DZ level). Optimized structures of nitrito-*κN* and nitrito-*κO* isomers of $[Pt(NMe_2C_2H_4NMeC_2H_4NMe_2)(NO_2)]^+$ and $[Pt(NO_2)_4]^{2-}$.

Table S1. Pt–N_{NO2} distances and dihedral angles between the coordination plane and nitrite ligand.

		Pt–N_{NO2} distances (Å)		Dihedral angle (°)	
Complex		100 K	180 K	100 K	180 K
1-Pt(NO₂)₄	N4 (cation)	2.005(2)	2.005(2)	74.0	74.5
	N5 (anion)	2.032(2)	2.030(2)	25.5	25.9
	N6 (anion)	2.014(3)	2.019(3)	67.1	66.8
	N7 (anion)	2.012(3)	2.007(3)	71.1	71.5
1-FSA		2.0094(15)	2.005(2)	83.3	82.1

Table S2. Reaction cavity volume surrounding the nitrile ligands (Å^3) before and after photoirradiation and conversion (%) in each site.

		Reaction cavity (Å^3)		Conversion (%, 180 K)		
Complex		100 K	180 K	1 h	4 h	13 h
1-Pt(NO₂)₄	N4 (cation)	1.63	1.52	29.8	42.9	48.8
	N5 (anion)	1.93	2.03	13.9	22.1	23.6
	N6 (anion)	32.7	34.0	42.7	59.4	65.3
	N7 (anion)	0.87	0.95	0	0	0
1-FSA		2.43	2.52	68.5	78.5	79.6

Table S3. Crystallographic parameters of **1-Pt(NO$_2$)$_4$** before and after photoirradiation at 100 K and 180 K

	1-Pt(NO$_2$)$_4$_100K	**1-Pt(NO$_2$)$_4$_180K_0h**	**1-Pt(NO$_2$)$_4$_180K_13h**
Empirical formula	$C_{26}H_{62}N_{12}O_{12}Pt_3$		
Formula weight	1320.14		
Crystal system	Monoclinic	Monoclinic	Monoclinic
Space group	*C*2/*c*	*C*2/*c*	*C*2/*c*
a [Å]	27.539(4)	27.5611(17)	27.713(2)
b [Å]	10.3539(14)	10.3835(7)	10.3236(9)
c [Å]	15.419(2)	15.5310(10)	15.7234(14)
β [°]	114.401(2)	114.4890(10)	114.6230(10)
V [Å^3]	4003.8(9)	4044.8(5)	4089.4(6)
Z	4	4	4
ρ_{calcd} [g cm^{-3}]	2.190	2.168	2.144
F(000)	2528	2528.0	2528.0
Temperature [K]	100	180	180
Reflns collected	11033	11204	11254
Independent reflns	4393	4448	4502
Parameters	246	246	330
R (int)	0.0179	0.0156	0.0258
R_1[a], R_w[b] ($I > 2\sigma$)	0.0162, 0.0392	0.0157, 0.0393	0.0367, 0.0781
R_1[a], R_w[b] (all data)	0.0175, 0.0397	0.0173, 0.0398	0.0431, 0.0802
Goodness of fit	1.073	1.035	1.103
$\Delta\rho_{max,min}$ [e Å^{-3}]	1.509, –1.241	1.387, –0.992	2.056, –1.864

[a] $R_1 = \Sigma||F_o| - |F_c|| / \Sigma|F_o|$. [b] $R_w = [\Sigma w (F_o^2 - F_c^2)^2 / \Sigma w (F_o^2)^2]^{1/2}$

Table S4. Crystallographic parameters of **1-FSA** before and after photoirradiation at 100 K and 180 K

	1-FSA_100K	**1-FSA_180K_0h**	**1-FSA_180K_13h**
Empirical formula	$C_{13}H_{31}F_2N_5O_6PtS_2$		
Formula weight	650.64		
Crystal system	Monoclinic	Monoclinic	Monoclinic
Space group	$P2_1/n$	$P2_1/n$	$P2_1/n$
a [Å]	11.0118(6)	11.0522(8)	11.2887(8)
b [Å]	15.7162(9)	15.7988(12)	15.7056(12)
c [Å]	12.7911(7)	12.8559(9)	12.8813(9)
β [°]	97.2260(10)	97.3320(10)	96.9970(10)
V [Å^3]	2196.1(2)	2226.4(3)	2266.8(3)
Z	4	4	4
ρ_{calcd} [g cm^{-3}]	1.968	1.941	1.906
F(000)	1280	1280.0	1280.0
Temperature [K]	100	180	180
Reflns collected	12262	12259	12456
Independent reflns	4828	4904	4987
Parameters	267	267	315
R (int)	0.0132	0.0397	0.0459
$R_1{}^a$, $R_w{}^b$ ($I > 2\sigma$)	0.0122, 0.0294	0.0230, 0.0618	0.0343, 0.0924
$R_1{}^a$, $R_w{}^b$ (all data)	0.0129, 0.0295	0.0246, 0.0627	0.0381, 0.0944
Goodness of fit	1.067	1.042	1.068
$\Delta\rho_{max,min}$ [e Å^{-3}]	0.679, –0.542	1.058, –0.831	2.145, –1.352

$^aR_1 = \Sigma||F_o| - |F_c|| / \Sigma|F_o|$. $^bR_w = [\Sigma w (F_o^2 - F_c^2)^2 / \Sigma w (F_o^2)^2]^{1/2}$